

Figure 3. Plot of $J\Delta^*P$ vs time.

The equality sign applies to steady state. Now, according to the generalization (20), we have

$$m = -(I\Delta^*\phi + J\Delta^*P) \geq 0 \quad (10)$$

Here the quantity $J\Delta^*P$ is that part of the rate of increase of dissipation function (11) which is due to change of the forces for the fixed values of the fluxes. According to the evolution criterion, the quantity is negative or zero (steady state) for any distance from equilibrium, provided the temperature is kept constant. The above conditions were maintained (approx-

mately) as the electrical potential difference is fixed and the total system is closed. Thus eq 10 can be reduced to eq 9, because $\Delta\phi$ is kept constant in these experiments. J and Δ^*P were evaluated from the slope of the curve obtained by plotting the rise of liquid against time, i.e., approach to steady state which was determined experimentally. In Figure 3 the values of $-J\Delta^*P$ for 20% and 60% acetonitrile + nitromethane mixtures are plotted at different intervals of time.

The curve approaches the time axis asymptotically, proving the theorem in the case of electroosmosis, and also it gives the evaluation of entropy production. Similar plots have been obtained in the case of the other compositions of the mixtures.

Registry No. CH_3CN , 75-05-8; nitromethane, 75-52-5.

Literature Cited

- (1) Rastogi, R. P.; Jha, K. M. *Trans. Faraday Soc.* **1966**, *62*, 585.
- (2) Rastogi, R. P.; Jha, K. M. *J. Phys. Chem.* **1966**, *70*, 1017.
- (3) Rastogi, R. P.; Singh, K.; Srivastava, M. L. *J. Phys. Chem.* **1969**, *73*, 46.
- (4) Rastogi, R. P.; Singh, K.; Singh, S. N. *J. Phys. Chem.* **1969**, *73*, 1593.
- (5) Rastogi, R. P.; Srivastava, M. L.; Singh, S. N. *J. Phys. Chem.* **1970**, *74*, 2960.
- (6) Blokhra, R. L.; Singal, T. C. *Indian J. Chem.* **1975**, *13*, 913.
- (7) Blokhra, R. L.; Parmar, M. L.; Sharma, V. P. *Colloid Interface Science*; Kerker, M., Ed.; Academic: New York, 1976; Vol. IV, p259.
- (8) Blokhra, R. L.; Parmar, M. L. *Indian J. Chem.* **1977**, *15A*, 384.
- (9) Hasse, R. *Thermodynamics of Irreversible Processes*; Addison-Wesley: Reading, MA, 1969.
- (10) Prigogine, I. *Introduction to Thermodynamics of Irreversible Process*; Wiley: New York, 1967.
- (11) Blokhra, R. L.; Parmar, M. L.; Agarwal, S. K. *J. Electroanal. Chem.* **1976**, *89*, 417.
- (12) Blokhra, R. L.; Agarwal, S. K.; Arora, Neeraj. *J. Colloid Interface Sci.* **1980**, *73*, 88.
- (13) Osterle, J. F. *J. Appl. Mech.* **1964**, *31*, 161.
- (14) Osterle, J. F. *J. Appl. Sci. Res.* **1964**, *12*, 425.
- (15) Morrison, F. A.; Osterle, J. F. *J. Chem. Phys.* **1965**, *43*, 211.
- (16) Kedam, O.; Caplan, S. R. *Trans. Faraday Soc.* **1965**, *61*, 1897.
- (17) Hasse, R. *Z. Phys. Chem. N.F.* **1976**, *103*, 235.
- (18) Hasse, R. *Z. Phys. Chem. N.F.* **1976**, *103*, 247.
- (19) Srivastava, R. C.; Blokhra, R. L. *Indian J. Chem.* **1963**, *1*, 156.
- (20) Glandsdroff, P.; Prigogine, I. *Physica's Grav.* **1954**, *20*, 773.

Received for review September 17, 1987. Accepted March 15, 1988.

Partial Miscibility Behavior of the Ethane + Propane + *n*-Dotriacontane Mixture

Susana S. Estrera and Kraemer D. Luks*

Department of Chemical Engineering, University of Tulsa, Tulsa, Oklahoma 74104-3189

The liquid-liquid-vapor partial miscibility of the mixture ethane + propane + *n*-dotriacontane is experimentally studied by using a visual cell (stoichiometric) technique. The ternary mixture, which has no constituent binary partial miscibility, has a liquid-liquid-vapor region bounded by upper and lower critical end point loci and a quadruple point locus (solid-liquid-vapor). The three-phase region extends from about 47 to 95 °C at pressures from 41 to 52 bar. The boundaries of the three-phase region are located in pressure-temperature space, and phase compositions and molar volumes of the three fluid phases are reported along isotherms at 50, 60, and 70 °C.

Introduction

The authors have undertaken an extensive study of phase equilibria behavior and liquid-liquid-vapor (LLV) immiscibility

phenomena in prototype rich gas + oil mixtures. "Rich gas", a mixture of methane + ethane + propane that has been separated from a live oil, is sometimes reinjected into reservoirs to enhance the recovery of the remaining oil. The purposes of the study are to map out the patterns of multiphase equilibria of these prototype mixtures in thermodynamic phase space and to generate a phase equilibria data base that would be useful for developing and testing equation-of-state models used to predict phase equilibria in and near regions of LLV immiscibility.

There is only limited immiscibility in binary mixtures of *n*-paraffins + methane, ethane, or propane. Partial miscibility has been observed in the mixtures methane + *n*-hexane (1) and methane + *n*-heptane (2, 3). *n*-Pentane is completely miscible with methane, while *n*-octane and higher members of the homologous series of *n*-paraffins are too molecularly dissimilar to methane to have a LLV region. Instead, a solid phase of the *n*-paraffin forms, creating two separate LV regions. The thermodynamic phase space topography of systems exhibiting

multiphase equilibria behavior has been reviewed by Luks and Kohn (4).

LLV immiscibility is seen in mixtures of ethane + *n*-paraffins ranging from *n*-octadecane to *n*-pentacosane (5–12). For carbon numbers 18 to 23, the LLV locus extends from a lower critical end point $L=L-V$ (LCST) to an upper critical end point $L-L=V$ (type K point), in the same manner as methane + *n*-hexane. For carbon numbers 24 and 25, the LLV locus is terminated below by the formation of a solid phase of the *n*-paraffin as a four-phase point SLLV (quadruple or Q point), as with methane + *n*-heptane.

LLV immiscibility in propane + *n*-paraffin mixtures does not commence until at least carbon number 37 (13, 14), presumably with a locus like that of methane + *n*-hexane or ethane + *n*-octadecane.

Given a LLV immiscible binary system, the addition of a second rich gas component, or "solvent", generates a LLV surface in thermodynamic phase space, with the binary locus as one boundary. The geometric nature of the ternary surface is governed by the nature of the second solvent relative to the components of the immiscible binary system (4, 15). It is possible, however, to have a ternary LLV surface without any of the constituent binary mixtures being LLV immiscible. One such ternary system is methane + ethane + *n*-octane (16). The three-phase region is bounded in pressure–temperature space by three loci, from above by a K-point locus, from below by a LCST locus, and at the lower temperatures by a Q-point locus, with the solid phase being *n*-octane. The region extends from about –75 to –51 °C. The K-point locus is close to the critical point ($L=V$) locus for methane + ethane in pressure–temperature space since *n*-octane is relatively nonvolatile at the three-phase LLV temperatures and thus resides predominantly in the lower (denser) L_1 liquid phase. The binary constituent mixture ethane + *n*-octane is completely miscible while, as stated above, the mixture methane + *n*-octane is too molecularly dissimilar to have a ternary LLV region. However, the proper proportion of methane-to-ethane is LLV immiscible with *n*-octane, thereby creating a LLV region in thermodynamic phase space.

The same situation will exist for a ternary system of ethane + propane + *n*-paraffin, for *n*-paraffins ranging from carbon number 26 to, say, 36. In this study we have chosen *n*-dotriacontane as the *n*-paraffin. Given its high triple point, one would expect *n*-dotriacontane to be essentially nonvolatile at the multiphase temperatures of interest, thereby creating a LLV region at and below the ethane + propane critical point locus in pressure–temperature space. We have experimentally mapped out the boundaries of the LLV region in this space and have detailed the compositions and molar volumes of the three fluid phases along three isotherms in the LLV region.

Experimental Apparatus and Procedures

A detailed description of the apparatus and some of the experimental procedures is given in earlier papers by Fall, Fall, and Luks (17–19). A visual cell (stoichiometric) technique was used for obtaining the pressure, temperature, phase compositions, and molar volumes of the ethane + propane + *n*-dotriacontane ternary system at 50, 60, and 70 °C. For a stoichiometric run, a known amount of *n*-dotriacontane liquid was added to a volume-calibrated visual glass cell (typically 7–9 mL in internal volume) using a heated syringe. Carefully measured amounts of the gases were then added to the cell from high-pressure bombs. By mass balances, the compositions and molar volumes of the three phases can be determined from "conjugate" measurements at a given temperature and pressure.

Conjugate measurements involve taking phase volume and overall composition raw data from three experimental runs in

which each phase in turn is volumetrically dominant relative to the two other phases. The necessary conjugate experiments therefore are an L_1 -dominant run, an L_2 -dominant run and a V -dominant run. Herein, the L_1 phase is that liquid phase richer in *n*-dotriacontane and is denser than the L_2 phase. For a ternary three-phase system, an invariant point requires that both the temperature and the pressure be fixed. Along a given isotherm, raw data were taken at various pressures and then plotted. Smoothing these raw data allowed the selection of specific pressures at the given temperature for mass balance analysis of the conjugate experiments (19). The vapor phase in all the experiments was assumed to contain no *n*-dotriacontane due to the low volatility of the hydrocarbon at the temperatures of interest.

The boundaries of the LLV region were determined by straightforward visual observation. Identification of these loci in pressure–temperature space was facilitated by a high-pressure adjustable-volume bomb which permitted the addition of compressed liquid propane to the visual cell at suitable overpressures (20).

Temperature was measured with a Pt resistance thermometer to an estimated accuracy of ± 0.02 K. Pressure was measured to ± 0.07 bar with pressure transducers which were frequently calibrated with a dead-weight gauge. Phase volumes in the calibrated visual cell were determined by a cathetometer to an accuracy of ± 0.005 mL.

Materials

The *n*-dotriacontane was purchased from Alfa Products with a stated purity of 99%. Its melting point in air was determined to be 69.22 ± 0.05 °C. This value compares favorably with that found in the literature (21). Chromatographic analysis of a solution of *n*-dotriacontane in *n*-decane also supported the stated purity.

The ethane was obtained from the Matheson Co. as a Research Purity Grade gas with a minimum rating of 99.93 mol %. The difference between the bubble point and dew point at 25 °C was less than 0.07 bar, and the vapor pressure at 50% liquid phase by volume was within ± 0.07 bar of the literature value (22). The propane was obtained from Air Products and Chemicals Inc., as an instrument grade gas with a minimum rating of 99.5 mol %. The difference between the bubble point and dew point at 25 °C was less than 0.07 bar and the vapor pressure at 50% liquid phase by volume was within ± 0.12 bar of the literature value (23).

The gases were first liquified in evacuated storage bombs cooled down to approximately 0 °C. In this two-phase condition, the vapor phase was vented and discarded to remove any light impurities. No further purification of the *n*-dotriacontane or the gases was performed.

Results

Table I presents pressure and temperature data for the LCST ($L=L-V$), $Q(S-L-L-V)$ -, and $K(L-L=V)$ -point loci which bound the three-phase LLV region of the mixture ethane + propane + *n*-dotriacontane. Figure 1 shows these data in $P-T$ space, along with the pure gas component vapor pressures (22, 23) and the critical locus for the mixture ethane + propane (24). These LCST, Q, and K point data should be good to ± 0.1 K and ± 0.07 bar. The intersections of the three-phase boundary loci in Figure 1 are not directly measured and should be as considered estimates.

The LLV data for the ethane + propane + *n*-dotriacontane system for isotherms at 50, 60, and 70 °C are presented in Table II. The molar compositions are estimated to be good to ± 0.009 and the liquid-phase molar volumes good to ± 7.0 mL/(g mol) at 50 °C. Vapor-phase molar volumes for this

Table I. Temperature and Pressure Raw Data for the Boundary Loci of Ethane + Propane + *n*-Dotriacontane

temp, K	press., bar	temp, K	press., bar
K Points			
322.87	51.49	348.56	51.06
323.29	51.50	349.68	50.99
327.34	51.76	352.91	50.53
329.95	51.78	356.24	49.93
335.46	51.89	357.83	49.84
335.65	51.81	357.89	49.77
339.26	51.55	358.98	49.65
345.00	51.41	362.15	49.04
Q Points			
320.57	42.61	321.05	44.26
320.81	43.43	321.46	47.22
320.83	43.42	321.67	49.18
LCST Points			
323.63	41.91	343.45	45.59
327.62	42.80	343.98	45.72
328.17	42.97	350.89	46.28
331.49	43.82	353.18	46.37
332.85	43.92	353.84	46.46
333.52	44.11	357.85	46.57
336.82	44.68	358.27	46.64
340.53	45.39	359.45	46.68

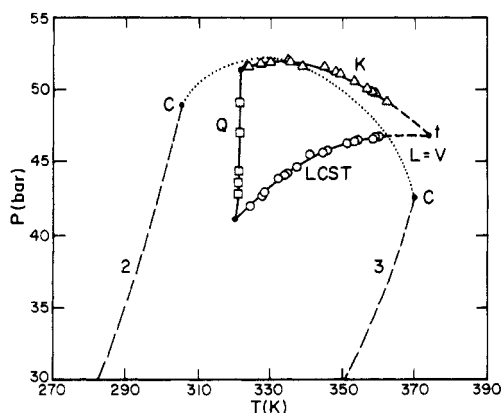


Figure 1. The liquid-liquid-vapor region of the system ethane + propane + *n*-dotriacontane in pressure-temperature space. Also shown are the critical point locus for the binary mixture ethane + propane (dotted curve) and the vapor pressure curves of pure ethane and propane (labeled 2 and 3).

isotherm should be reliable to $\pm 6\%$ of the reported values at all pressures. For the 60 °C isotherm, the molar compositions should be good to ± 0.06 and the liquid-phase molar volumes good to ± 7.0 mL/(g mol). Vapor-phase molar volumes for this isotherm should be reliable to $\pm 2.5\%$ of the reported values at all pressures. The molar compositions should be good to ± 0.004 and the liquid-phase molar volumes good to ± 3.0 mL/(g mol) at 70 °C. Vapor-phase molar volumes for this isotherm should be within $\pm 1\%$ of the reported values at all pressures. All these estimates are based on average absolute deviations (AAD) of the calculated LLV phase properties of several replicate experimental runs. Plots of the LLV behavior of this system at 50 °C are presented in Figures 2, 3, and 4. Figures 2 and 3 plot liquid- and vapor-phase compositions against pressure, while Figure 4 plots the liquid-phase molar volumes versus pressure.

Remarks

The three-phase liquid-liquid-vapor region for ethane + propane + *n*-dotriacontane has considerable range, extending from about 47 °C, where a solid phase of *n*-dotriacontane

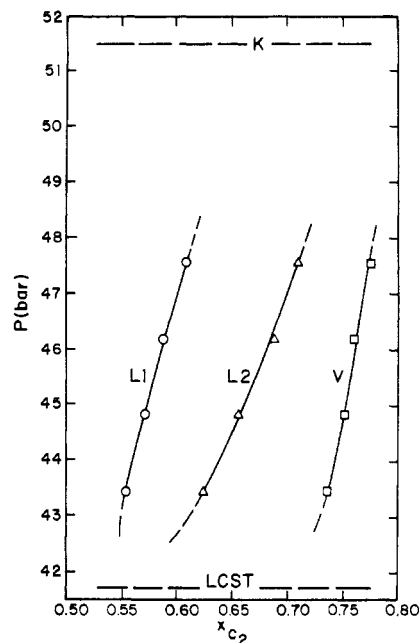


Figure 2. Ethane mole fraction as a function of pressure for the liquid-liquid-vapor region of ethane + propane + *n*-dotriacontane at 50 °C.

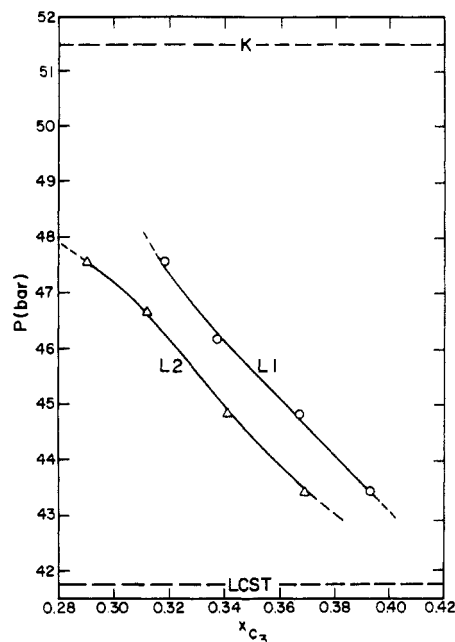


Figure 3. Propane mole fraction as a function of pressure for the liquid-liquid-vapor region of ethane + propane + *n*-dotriacontane at 50 °C.

forms at the Q-phase locus, to approximately 95 °C where there will be a tricritical (invariant) point ($L=L=V$). As anticipated, the K-point boundary of the region is located close to the critical point locus ($L=V$) of the binary mixture ethane + propane, since the binary LV system is compositionally similar to the L_2 and V phases of the ternary system. This large LLV region extent can possibly be accounted for by the fact that *n*-dotriacontane is roughly midway between carbon numbers 26 and 37, the numbers bounding binary LLV immiscibility of *n*-paraffins with ethane (upper limit) and propane (lower limit), respectively. A similar phenomenon was seen with the ternary homologous series nitrogen + methane + *n*-paraffins. The

Table II. Pressure, Phase Compositions, and Molar Volumes for the Liquid-Liquid-Vapor Region of Ethane + Propane + *n*-Dotriacontane

press., bar	L ₁ phase		mol vol, mL/(g mol)	L ₂ phase		mol vol, mL/(g mol)	V phase	
	mole fracn			mole fracn			mole fracn	mol vol, mL/(g mol)
	C ₂	C ₃		C ₂	C ₃		C ₂	
Temperature = 50 °C (323.15 K)								
41.71 ^a								
43.44	0.5531	0.3926	108.7	0.6237	0.3692	96.6	0.7353	308.1
44.82	0.5697	0.3668	111.2	0.6540	0.3410	97.8	0.7501	291.2
46.19	0.5861	0.3424	114.1	0.6854	0.3111	99.5	0.7595	271.2
47.57	0.6053	0.3167	116.8	0.7077	0.2893	101.8	0.7747	251.9
51.50 ^b								
Temperature = 60 °C (333.15 K)								
44.20 ^a								
44.82	0.4477	0.5055	110.3	0.4875	0.5034	106.3	0.5999	302.3
46.19	0.4622	0.4800	112.1	0.5164	0.4788	109.8	0.6195	282.0
47.57	0.4864	0.4519	114.1	0.5494	0.4469	111.2	0.6309	262.2
51.78 ^b								
Temperature = 70 °C (343.15 K)								
45.64 ^a								
47.67	0.4123	0.5421	105.0	0.4482	0.5469	105.6	0.5328	252.1
48.95	0.4261	0.5227	103.9	0.4801	0.5170	109.2	0.5485	229.8
51.37 ^b								

^aLCST point. ^bK point.

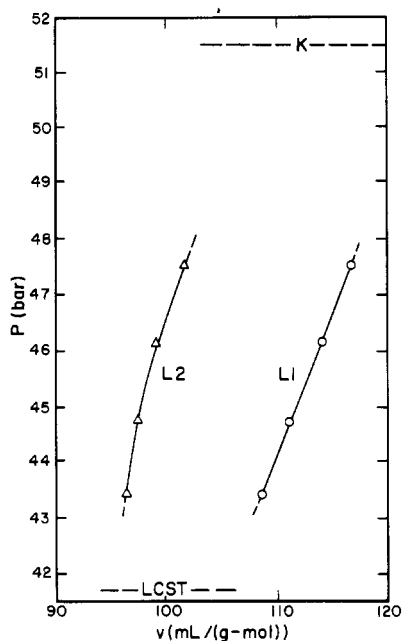


Figure 4. Molar volume as a function of pressure for the L₁ and L₂ phases for the liquid-liquid-vapor region of ethane + propane + *n*-dotriacontane at 50 °C.

largest three-phase LLV region in pressure-temperature space occurred with *n*-butane, intermediate to propane and *n*-hexane, which are the *n*-paraffins that bound binary LLV immiscibility with nitrogen and methane, respectively (25).

Two comments should be made about the error, or reliability, estimates of the isothermal LLV data presented in the preceding section. First of all, the data at the lower temperatures have more scatter due, we judge, to the occasional formation of solid *n*-dotriacontane in constrictions in the vapor-phase region of the visual cell. These difficulties diminished with increasing temperature. Second, the error estimates are larger in this study than in the earlier study of Fall and Luks (19) using a similar experimental apparatus. The precision or reproducibility of the data depends on one's ability to perform mass balances of a "lever principle" nature. In this present study, the phases L₁ and L₂ are more closely matched in properties than they are for the carbon dioxide-containing systems in ref 19. Conse-

quently it is more difficult to distinguish, propertywise, between the liquid phases in this present study, resulting in larger error estimates, given a fixed uncertainty in any measurement, say, the volume of a phase. The property AAD's appear to be inversely proportional to the property differences between L₁ and L₂ when this study is compared with ref 19.

Glossary

AAD	average absolute deviation
C	a pure component critical point where L=V
K	a K point, a critical end point where L-L=V
L, L ₁ , L ₂	liquid phases
LCST	a lower critical end point where L=L-V
Q	a Q point, or quadruple point, which has four phases in equilibria; herein, the four phases are SLLV
t	a tricritical point where L=L=V
V	vapor phase

Registry No. *n*-Dotriacontane, 544-85-4; ethane, 74-84-0; propane, 74-98-6.

Literature Cited

- Lin, Y. N.; Chen, R. J. J.; Chappellear, P. S.; Kobayashi, R. *J. Chem. Eng. Data* **1977**, *22*, 402-408.
- Kohn, J. *AIChE J.* **1961**, *7*, 514-518.
- Chang, H. L.; Hurt, L. J.; Kobayashi, R. *AIChE J.* **1966**, *12*, 1212-1216.
- Luks, K. D.; Kohn, J. P. *Proceedings of the 63rd Annual Convention Gas Processors Association, New Orleans, LA, March 21, 1984*; Gas Processors Association; Tulsa, OK, 1984; pp 181-186.
- Kohn, J. P.; Kim, Y. J.; Pan, Y. C. *J. Chem. Eng. Data* **1966**, *11*, 333-335.
- Specovius, J.; Leiva, M. A.; Scott, R. D.; Knobler, C. M. *J. Phys. Chem.* **1981**, *85*, 2313-2316.
- Rodrigues, A. B.; Kohn, J. P. *J. Chem. Eng. Data* **1967**, *12*, 191-193.
- Patel, A. D. M.S. Thesis, University of Notre Dame, Aug. 1966.
- Peters, C. J.; Lichtenthaler, R. N.; de Swaan Arons, J. *Fluid Phase Equilib.* **1986**, *29*, 495-504.
- Estrera, S. S.; Luks, K. D. *J. Chem. Eng. Data* **1987**, *32*, 201-204.
- Peters, C. J.; de Roo, J. L.; de Swaan Arons, J. *J. Chem. Thermodyn.* **1967**, *19*, 265-272.
- Peters, C. J.; Van Der Kool, H. J.; de Swaan Arons, J. *J. Chem. Thermodyn.* **1967**, *19*, 395-405.
- Rowlinson, J. S.; Freeman, P. I. *Pure Appl. Chem.* **1961**, *2*, 329-334.
- Leder, F.; Irani, C. A.; McHenry, J. A. *AIChE J.* **1976**, *22*, 199-200.
- Luks, K. D. *Fluid Phase Equilib.* **1986**, *29*, 209-224.
- Hottovy, J. D.; Kohn, J. P.; Luks, K. D. *J. Chem. Eng. Data* **1981**, *26*, 135-137.
- Fall, D. J.; Luks, K. D. *J. Chem. Eng. Data* **1984**, *29*, 413-417.
- Fall, D. J.; Fall, J. L.; Luks, K. D. *J. Chem. Eng. Data* **1985**, *30*, 82-88.

- (19) Fall, J. L.; Luks, K. D. *J. Chem. Eng. Data* **1986**, *31*, 332-336.
 (20) Estrera, S. S. Ph. D. Dissertation, University of Tulsa, 1987.
 (21) Weast, R. C. *Handbook of Chemistry and Physics*, 51st ed.; The Chemical Rubber Co.: Boca Raton, FL, 1970; pp C53-542.
 (22) Goodwin, R. D.; Roder, H. M.; Straty, G. C. *Natl. Bur. Stand. Tech. Note* **1976**, No. 684, 58-61.
 (23) Goodwin, R. D.; Haynes, W. M. *Natl. Bur. Stand. Monograph* **1982**, No. 170, 55-59.
 (24) Djordjević, L.; Budenholzer, R. A. *J. Chem. Eng. Data* **1970**, *15*, 10-12.

- (25) Liave, F. M.; Luks, K. D.; Kohn, J. P. *J. Chem. Eng. Data* **1987**, *32*, 14-17.

Received for review September 22, 1987. Accepted February 11, 1988. Support of this research was provided by The National Science Foundation (Grant No. CBT-8514599). The apparatus used is part of the PVTx Laboratory at the University of Tulsa and was purchased with funds provided by several industries, The University of Tulsa, and a National Science Foundation specialized equipment grant (No. CPE-8104650).

Apparent Molar Heat Capacity and Other Thermodynamic Properties of Aqueous KCl Solutions to High Temperatures and Pressures

Roberto T. Pabalan and Kenneth S. Pitzer*

Lawrence Berkeley Laboratory and Department of Chemistry, University of California, Berkeley, California 94720

Heat capacities of KCl solutions have been measured from 413 to 573 K at 200 bar over the molality range of 0.05-3.0 mol kg⁻¹. These were combined with literature data on volumes, heat capacities, enthalpies, and osmotic coefficients up to a temperature of 599 K and a pressure of 500 bar to yield comprehensive equations for the calculation of the thermodynamic properties of KCl(aq) to high temperatures and pressures by using the ion-interaction approach of Pitzer.

Introduction

Potassium chloride is an important electrolyte in many natural and industrial waters and its thermodynamic properties are of practical interest in industrial and geochemical applications. Heat capacities are particularly useful since these can be integrated to yield enthalpy and activity data by using integration constants evaluated from 298 K data available in the literature. Recent developments in flow calorimetry have minimized the experimental problems associated with determining heat capacities and have provided a useful tool for investigating the thermodynamic properties of electrolyte solutions to elevated conditions of temperature and pressure.

In this study we report our results for the heat capacity of KCl (aq) solutions at molalities from 0.05 to 3.0 mol kg⁻¹ and temperatures from 413 to 573 K at a pressure of 200 bar. These values are combined with literature data on heat capacities, osmotic coefficients, and volumes to get a comprehensive set of equations for describing the thermodynamic properties of KCl (aq) to high temperatures and pressures.

Experimental Section

The heat capacity of KCl solutions were measured with a flow calorimeter described in detail by Rogers and Pitzer (1) and modified by Phutela and Pitzer (2). This high-temperature flow calorimeter is an adaptation of the design used by Picker et al. (3).

Briefly, the system consists of two flow calorimetric cells within the same thermostat plus two liquid-chromatography pumps (Kratos Spectroflow 400). In normal operations only one pump is used, and the flow is in series through the two cells. In calibration runs water flows through both cells. For solution measurements one has an exactly equal volumetric flow rate of water to one cell, and solution to the other. With both the sample solution and pure water flowing in the calo-

rimeter, the electrical power necessary to equalize the temperature rise in both sides of the calorimeter is measured. The specific heat capacity of the solution at constant pressure, $c_{p,s}$, is then given by

$$c_{p,s}/c_{p,w} = \{1 + f(P_s - P_w)/P_w\} \rho_{w,298K} / \rho_{s,298K} \quad (11)$$

where $c_{p,s}$ and $c_{p,w}$ are the specific heat capacities of the solution and of pure water, respectively, f is the heat-loss correction factor, P_s and P_w are the electrical powers for solution and water, respectively, and $\rho_{w,298K}$ and $\rho_{s,298K}$ are the densities at 298.15 K of water and solution, respectively.

The correction factors were evaluated at each temperature by using a method suggested by Picker et al. (3) and used by Fortier et al. (4) and Smith-Magowan and Wood (5), with water flowing through both sides of the calorimeter and mimicking a change in the heat capacity on the working side by adding an increment of water flow through that side. For this purpose the second Spectroflow 400 pump was connected to the working side of our calorimeter.

The apparent molar heat capacity, ${}^\phi C_p$, can be calculated from the equation

$${}^\phi C_p = c_{p,s} M_2 + 1000(c_{p,s} - c_{p,w})/m \quad (12)$$

where m and M_2 are the molality and molecular weight of KCl, respectively.

The solutions used in this study were made up by mass from Baker reagent-grade KCl, which was dried overnight at 473 K and cooled in a vacuum desiccator.

Experimental Results

The results of the heat capacity measurements on KCl solutions are given in Table I. All of the present results are for 200 bar. Water properties used in the calculations were derived from the equation of state of Haar et al. (6), while the densities of KCl solutions at 298.15 K and 200 bar were obtained from the fit of Gates and Wood (7). The error estimates given in Table I were calculated from our sensitivity limit in determining P_s/P_w , typically ± 0.00015 , and an accuracy of $\pm 1\%$ in the measurement of $(P_s - P_w)/P_w$ and of the correction factor, f .

Calculations

Review of Equations. One of our goals is to generate a comprehensive set of equations which describe the thermodynamic properties of aqueous KCl from these heat capacities and other appropriate data. The system of equations chosen